

1 **Hepatitis C virus infection inhibits P-body granule formation in human livers**

2

3 Gemma Pérez-Vilaró¹⁺, Carlos Fernández-Carrillo²⁺, Laura Mensa², Rosa Miquel³,

4 Xavier Sanjuan^{4,5}, Xavier Forns², Sofía Pérez-del-Pulgar^{2*}, Juana Díez^{1*}

5

6 ¹Molecular Virology, Universitat Pompeu Fabra, Barcelona, Spain

7 ²Liver Unit, Hospital Clínic, IDIBAPS, CIBERehd, Barcelona, Spain

8 ³Pathology Department, Hospital Clínic, Barcelona, Spain

9 ⁴Scientific and Technical Services, Universitat Pompeu Fabra, Barcelona, Spain

10 ⁵Advanced Light Microscopy Unit, Center for Genomic Regulation, Barcelona, Spain

11 ⁺Authors share co-first authorship

12 ^{*}Authors share co-senior authorship

13 To whom correspondence should be addressed:

14 **Juana Díez, PhD**

15 Molecular Virology Group

16 Department of Experimental and Health Sciences

17 Universitat Pompeu Fabra

18 Doctor Aiguader, 88, 08003 Barcelona, Spain

19 Phone. +34-933 160 862 / Fax. +34-933 160 901

20 E-mail: juana.diez@upf.edu

21 **Sofía Pérez-del-Pulgar, PhD**

22 Hospital Clínic, IDIBAPS, CIBERehd

23 Rossellón 149-153, 08036 Barcelona, Spain

24 Phone. +34 932275400 (2093) / Fax. +34 933129405

25 E-mail: sofiapp@clinic.ub.es

26

27 **Electronic word count:** 4795 words including the abstract, references, tables and figure
28 legends.

29 **Number of figures and tables:** 4 Figures, 1 Table

30 **Abbreviations used in this paper:** HCV, hepatitis C virus; P-bodies, processing
31 bodies; HBV, hepatitis B virus.

32 **Keywords:** P-bodies; HCV; *in vivo*; liver

33 **Conflicts of interest:** The authors who have taken part in this study declared that they
34 do not have anything to disclose regarding funding or conflict of interest with respect to
35 this manuscript.

36 **Financial support:** JD and GPV were supported by a grant from the Spanish Ministry
37 of Economy and Competitiveness (BFU2013-44629-R). XF received support in part by
38 a grant from Instituto de Salud Carlos III (PI11/01907), Ministerio de Economía y
39 Competitividad, co-funded by Fondo Europeo de Desarrollo Regional, Unión Europea,
40 Una manera de hacer Europa. XF and SPP also received a grant from the Roche Organ
41 Transplantation Research Foundation (ROTRF, CI: 442035057). The other authors were
42 supported by grants from the following institutions: CFC from Asociación Española
43 para el Estudio del Hígado and LM from Instituto de Salud Carlos III, Ministerio de
44 Economía y Competitividad.

45 **Author's Contributions:** GPV and CFC designed, performed experiments and
46 analyzed data; CFC collected clinical data; CFC and LM set up conditions for the
47 immunostaining of P-body components in formalin-fixed paraffin-embedded liver
48 biopsies; XS provided technical assistance and acquired images for 3D reconstruction
49 experiments; RM did the histopathological processing and diagnostic analysis of liver
50 tissue samples; JD, SPP and XF supervised all aspects of this study, including design,
51 execution, data analysis, interpretation and manuscript preparation; JD came up with the
52 research idea; XF provided the patient cohort and the clinical samples; JD and GPV

53 wrote the manuscript; All authors contributed to the interpretation and discussion of the
54 results, as well as to the revision of the manuscript.

55

56

57

58

59

60

61

62

63

64

65

66

67

68

69

70

71

72

73

74

75

76

77

78 **Abstract**

79 **Background & Aims:** Decoding the myriad of interactions that Hepatitis C virus
80 (HCV) establishes with the infected cells is mandatory to obtain a complete
81 understanding of HCV biology and its associated pathogenesis. We and others have
82 previously identified in cell culture that HCV infection disrupts the formation of P-
83 bodies. These are cytoplasmic RNA granules with key roles in post-transcriptional
84 regulation of gene expression. Consequently, P-body disruption might have
85 consequences beyond viral propagation. However, whether P-body disruption occurs
86 also *in vivo* is unknown. Aim of this study was to address this important issue.

87 **Methods:** Formalin-fixed paraffin-embedded liver biopsies from 4 groups of patients
88 (healthy donors, patients with non-virus related liver inflammation, HCV- and HBV-
89 infected patients) were immunostained to detect DDX6 and Dcp1, two core P-body
90 components. Changes in the localization of these proteins were assessed by confocal
91 microscopy.

92 **Results:** HCV specifically inhibited P-body formation in hepatocytes from human
93 livers regardless of viral genotype, inflammation grade or whether the infection was
94 recent or long established. Importantly, this alteration was reversed once HCV is
95 eliminated by therapy. Furthermore, *in vivo* an unexpected heterogeneity in P-body
96 composition was observed that might reflect functional specializations.

97 **Conclusions:** This is the first comprehensive P-body analysis *in vivo* that links a
98 pathogenic condition to P-body alterations. Given the role of P-bodies in cellular gene
99 expression, their alteration should be considered to fully understand the complex HCV-
100 associated pathologies.

101 **Abstract word count:** 229 words

102 **Keywords:** P-bodies; HCV; *in vivo*; liver

103 **Introduction**

104 Hepatitis C virus (HCV) remains a major threat for human health. Around 130-170
105 million people worldwide are chronically infected and at high risk to develop liver
106 fibrosis, cirrhosis and hepatocellular carcinoma [1]. There is no vaccine against HCV
107 and the recently approved treatments, although increasingly effective, are genotype
108 specific, expensive, and present multiple side effects and contraindications [2, 3]. Thus,
109 it is of interest to expand the therapy options against HCV. For this, it is necessary to
110 gain a deeper knowledge of the HCV life cycle.

111

112 All steps of the HCV life cycle involve interactions between few HCV components and
113 a myriad of host factors. Over the last years major advances have been made in the
114 identification of such interactions using a robust HCV cell culture system that uses a
115 virus strain isolated from a patient with fulminant hepatitis, a rare event in HCV
116 infections [4], and Huh7 hepatoma cell lines [5]. However, although very useful, this is
117 an artificial system that does not recapitulate the host environment that HCV faces in
118 chronic infected livers. Moreover, Huh7 cells are transformed cells with an impaired
119 innate antiviral response [6]. Consequently, *in vivo* studies in the infected human liver
120 are essential to determine the relevance of identified host-HCV interactions.

121

122 Cell compartmentalization ensures the timely and quantitative provision of molecules in
123 the cytoplasm of eukaryotic cells. These compartments include classical among others
124 membrane organelles such as the endoplasmic reticulum and more recently identified
125 membrane-less RNA granules named P-bodies. By using the HCV cell culture system
126 we and others have shown that HCV not only manipulates host membranes but also P-
127 bodies [7, 8]. P-bodies are involved in post-transcriptional regulation of gene
128 expression. They are highly dynamic and contain translationally silent mRNAs together

129 with multiple proteins from the mRNA decay and silencing machineries [9, 10]. Once in
130 P-bodies, mRNAs can be either degraded or stored for a later return into translation [11-
131 13]. HCV hijacks the core P-body components PatL1, Lsm1-7 and DDX6 (also referred
132 as Rck/p54), that are required for P-body formation, to efficiently translate and replicate
133 its RNA genome [14]. This is associated with a significant reduction in the number of
134 P-bodies within infected cells, presumably by keeping the required components away
135 from participating in P-body formation since PatL1, Lsm1-7 and DDX6 expression is
136 not changed [7, 8]. Alterations in P-body components and P-body formation might have
137 consequences *in vivo* beyond HCV propagation. Indeed, such alterations not only have
138 been connected to other viral infections but also to stress conditions and to cancer [15-
139 19]. However, as for HCV, all these connections have been derived from indirect
140 evidences and cell culture studies.

141

142 Here we show that HCV specifically decreases P-body abundance in hepatocytes from
143 human livers. This is the first direct link *in vivo* between a pathogenic condition and P-
144 body alterations.

145

146 **Materials and Methods**

147 *Patients*

148 A total of 55 patients were selected for this study, all of them attending the Hospital
149 Clínic of Barcelona between 2002 and 2013. All patients provided written informed
150 consent to use their liver samples. Our study was approved by the Ethics Committee of
151 Hospital Clínic of Barcelona, in accordance with the guidelines set forth in the 1975
152 Declaration of Helsinki. Liver biopsies were performed from patients when clinically
153 indicated. Aiming to assess changes in P-bodies during HCV infection, we studied 19
154 HCV chronically-infected immunocompetent patients with a liver biopsy done before

155 antiviral treatment (**Table 1**). Most of these patients showed typical histological features
156 of chronic hepatitis with variable degree of periportal and/or lobular necroinflammation.
157 As HCV-negative control group, 10 healthy donors for living donor liver transplantation
158 (designated as healthy donors in the main text) were selected. To compare HCV
159 infection with another viral hepatitis, we also enrolled 8 chronically HBV-infected
160 immunocompetent patients with a liver biopsy performed before antiviral treatment.
161 Most of the HBV-infected patients showed histological features of chronic hepatitis. In
162 order to address a possible influence of inflammation *per se* on P-bodies, we selected 10
163 HCV- and HBV-negative liver transplant (LT) patients showing inflammatory changes
164 at the liver biopsy due to non-viral causes, mainly transplant rejection. Most of the non-
165 viral LT patients had portal lymphoid inflammatory infiltrates associated with variable
166 lobular inflammation. The clinical and histological characteristics of the 3 control
167 groups are summarized in **Supplementary Table 1**. To test the reversibility of P-body
168 changes after HCV clearance, we also selected 3 patients who received antiviral
169 treatment after LT and achieved a sustained virological response (demonstrated by
170 negative PCR tests immediately after and at 6 months after treatment). In this group,
171 liver biopsies were obtained before and after HCV clearance. To assess P-body changes
172 in acute HCV infection we selected another 3 patients with hepatitis C recurrence after
173 LT who were biopsied during acute phase hepatitis (0.5 and 6 months after LT).
174 Colocalization studies with HCV core protein and DDX6 were performed in biopsies
175 obtained from 2 patients with HCV recurrence after LT and very high viral load (7.7
176 and 8.0 log₁₀ IU/mL, respectively).

177

178 *Histopathological processing and diagnostic analysis of liver tissue samples*

179 Tissue specimens were formalin-fixed, paraffin-embedded (FFPE) and stained with
180 hematoxylin-eosin and Mason's trichrome as routinely done for diagnostic purposes in

181 the Pathology Department at the Hospital Clínic of Barcelona. Samples were analyzed
182 by an expert liver pathologist (RM). Chronic viral hepatitis was graded and staged by
183 the METAVIR score system [20]. Routine methods and scoring systems were used to
184 characterize histopathological findings according to other specific clinical conditions
185 (Banff recommendations for rejection, etc.; **Supplementary Table 1**).

186

187 *Indirect immunofluorescence*

188 Five-micrometer sections were cut from paraffin blocks and mounted onto charged
189 slides. The slides were heated overnight at 37°C and then subjected to antigen retrieval
190 using the PT Link automated system (Dako, Glostrup, Denmark). Antigen retrieval
191 conditions were high pH buffer, no preheat mode, target retrieval mode at 97°C for 20
192 minutes. The sections were afterwards blocked with phosphate-buffered saline (PBS) /
193 10% goat serum (Jackson ImmunoResearch, PA, USA) during 30 minutes. Incubation
194 with primary antibodies was performed at room temperature during 120 minutes. The
195 primary antibodies used were 5 µg/mL rabbit polyclonal anti-DDX6/rck (p54) (MBL,
196 Nagoya, Japan), 1.3 µg/mL mouse monoclonal IgG1 anti-DDX6 3D2 (Sigma-Aldrich,
197 MO, USA), 0.8 µg/mL mouse monoclonal IgG2a anti-Dcp1A 3G4 (Abnova, Taipei,
198 Taiwan) and 1 µg/mL mouse monoclonal IgG1 anti-core C7-50 (Santa Cruz
199 Biotechnology, CA, USA). After incubation with the primary antibodies, sections were
200 washed three times with PBS (5 minutes each) and incubated with the secondary
201 antibody for 1 hour at room temperature. The secondary antibodies used were 2 µg/mL
202 Alexa Fluor® 647 goat anti-rabbit IgG and Alexa Fluor® 568 goat anti-mouse IgG
203 (Invitrogen, CA, USA). After the second incubation, 3 additional washes with PBS
204 were performed and the slides were incubated again for 5 minutes with 1 µg/mL DAPI
205 (Sigma-Aldrich, MO, USA) followed by three final washes with PBS and once with

206 deionized water. Finally, the samples were mounted with ProLong® Gold Antifade
207 Reagent (Invitrogen, CA, USA).

208

209 *Confocal imaging and data analysis*

210 Images were acquired with a Leica TCS SP5 confocal microscope using a 63× 1.4-NA
211 PL APO objective (Leica Microsystems GmbH). For each liver biopsy 10 different non-
212 overlapping fields were analyzed. Portal spaces were systematically excluded, avoiding
213 areas of high lymphocyte concentration or poor DAPI quality staining. In total, more
214 than 200 hepatocytes were analyzed per biopsy. Image processing and analysis to obtain
215 the number and size of DDX6- and Dcp1-containing P-bodies was performed with Fiji
216 software [21]. Areas with liver sinusoids and/or lipofuscin aggregates were excluded
217 from the analysis by masking them. The resulting images were processed by using a
218 difference-of-Gaussians filter to enhance structures within the range of the two
219 Gaussians (sigma 0.5 and 2). Filtered images were subsequently thresholded for P-body
220 particles segmentation and counting. The number of hepatocytes per field was obtained
221 by counting nuclei within a specified range in size (500-5000 pixels) and circularity
222 (0.85-1.00) and final values for P-body counts per hepatocyte were obtained from
223 relating the number of P-bodies in each image to the number of hepatocytes. In the
224 indicated experiments, Z-stacks at the optimal Nyquist axial step size (0.13 µm) from at
225 least 30 randomly selected cells under each condition were collected. Stacks were
226 analyzed to obtain P-body numbers in a similar way as described above, yet using tools
227 to process, threshold and count volumes instead of areas. To perform 3D
228 reconstructions, Z-stacks were deconvolved using Huygens Essential 4.1 software
229 (Scientific Volume Imaging BV, Hilversum, The Netherlands) and visualized with
230 isosurfaces using Imaris 64X 7.6.4 software (Bitplane AG, Zurich, Switzerland).

231

232 *Statistical analysis*

233 Mann-Whitney *U* test was performed when comparing quantitative variables in
234 unpaired groups. Wilcoxon signed-rank test was used to compare quantitative variables
235 in paired groups. A two-tailed p-value of less than 0.05 was considered statistically
236 significant. Data were analyzed with SPSS Statistics 20 (IBM) and Prism 5.01
237 (GraphPad) software.

238

239 **Results**

240 *HCV infection specifically decreases P-body abundance in livers from chronically*
241 *infected patients*

242 We have previously reported that HCV utilizes P-body components to propagate and
243 induce granule disruption in cell culture [7, 14]. These *in vitro* results encouraged us to
244 investigate whether HCV infection affects P-body formation in the liver of chronically
245 infected patients. For this, formalin-fixed paraffin-embedded liver biopsies from HCV-
246 infected patients (n=19, **Table 1**) and healthy donors (n=10) were double
247 immunostained to detect the two core P-body components DDX6 and Dcp1. P-body
248 detection was assessed by confocal microscopy (**Fig. 1A**). Regardless of the infecting
249 HCV genotype (1a, 1b, 2, 3 or 4) or the inflammation grade, the abundance of P-bodies
250 containing DDX6 and Dcp1 were reduced by ~2- and ~10-fold, respectively, in
251 hepatocytes from HCV-infected patients relative to hepatocytes from healthy donors
252 (**Fig. 1B**). The number of Dcp1-positive P-bodies in the biopsies from healthy
253 individuals exhibited a wide variation among samples that was narrowed down in the
254 presence of HCV infection.

255 To determine whether the observed alterations were HCV-specific we included in our
256 study liver biopsies from patients chronically infected with hepatitis B virus (HBV)
257 (n=8) and from patients with non-virus related inflammatory changes (n=10). The first

258 group of patients allowed determining whether another virus infection that targets the
259 liver could also lead to P-body disruption, while the second group allowed addressing
260 the putative role of liver inflammation in P-body alterations. Importantly, no decrease in
261 the number of P-bodies containing DDX6 was observed in liver biopsies from HBV-
262 infected patients or with non-virus related inflammatory changes. Likewise, the values
263 obtained for P-bodies containing Dcp1 in these patients were disperse and no significant
264 differences were observed when compared to healthy donors (**Fig1. B**). Thus *in vivo*
265 HCV infection specifically decreases P-body abundance.

266

267 *The effect of HCV on P-body disruption occurs in both acute and chronic infections and*
268 *is reversed once HCV is eliminated by therapy*

269 To assess whether a reduced P-body abundance is reversibly linked to HCV infection,
270 we longitudinally analysed P-bodies in liver biopsies from chronically infected patients
271 before and after antiviral treatment (n=3), once a sustained virological response and thus
272 viral clearance had been achieved. In all cases, the number of P-bodies per hepatocyte
273 containing DDX6 or Dcp1 increased upon viral clearance, reaching levels comparable
274 to the ones found in healthy donors (**Fig. 2**). Of note is that although the number of P-
275 bodies per hepatocyte seemed patient specific, the ratio between P-body numbers
276 obtained before and after antiviral treatment was similar among the three patients
277 analysed.

278 To determine whether the HCV-induced changes in P-bodies from hepatocytes require a
279 chronic state of the viral infection or also occurs in acute states, we analyzed biopsies
280 from liver transplant patients with acute recurrent hepatitis C (n=3), which mimics the
281 initial phase of the infection. In these biopsies the number of P-bodies that contained
282 DDX6 or Dcp1 was similar to the ones found in chronically infected patients (**Fig. 2**).

283 Collectively, although the amount of samples was limited, these results support that
284 HCV infection, acute or chronic, specifically decreases P-body abundance and that this
285 decrease is reversed once HCV is eliminated by therapy.

286

287 *In vivo, P-body granules in somatic cells are more heterogeneous than previously*
288 *anticipated*

289 The composition and formation of P-bodies in somatic cells *in vivo* is mostly
290 unexplored since available studies have focused on cell culture systems [11, 12].
291 Interestingly, analyses of the liver images from confocal microscopy revealed
292 unexpected peculiarities. There was no colocalization of DDX6 and Dcp1 in
293 hepatocytes *in vivo* although such colocalization is commonly observed in hepatoma
294 cell lines, like Huh 7.5, used to study HCV *in vitro* [7]. This lack of colocalization was
295 hepatocyte-specific since parenchyma-infiltrating lymphocytes of the same individual
296 showed a strong colocalization of DDX6 and Dcp1 (**Fig. 3**). Thus, *in vivo*, P-body
297 granules seem to be more heterogeneous than previously anticipated *in vitro* and cell-
298 type specific.

299

300 *3D single cell analyses corroborates the P-body number decrease observed at a global*
301 *level in HCV-infected livers*

302 Confocal analysis allows the acquisition of single cell sections. To eliminate the
303 possibility that the P-body changes in HCV chronically infected livers were due to
304 alterations in P-body intracellular distribution, we carried out detailed single-cell 3D
305 analyses. Liver biopsies from patients with severe HCV recurrence after liver
306 transplantation were double immunostained for the HCV core protein and the P-body
307 component DDX6. Double staining with the HCV core antigen ensured that only HCV-
308 infected cells were analyzed. The use of biopsies from liver transplant patients with high

309 viral load and, therefore, high HCV antigen levels allowed overcoming the experimental
310 limitations of the low abundance of HCV antigens in infected cells and the unfavorable
311 imaging properties of the liver [22]. Z-stack images were obtained and P-body
312 abundance and intracellular localization was evaluated and compared with that in
313 hepatocytes from healthy donors. DDX6-containing P-bodies were reduced by ~2-fold
314 in core-positive hepatocytes from HCV-infected patients relative to hepatocytes from
315 healthy donors (**Fig. 4A**). This value parallels the one obtained with single stack
316 analyses where infected and non-infected hepatocytes are indistinguishable (**Fig. 1B**). In
317 line with this, when P-bodies were quantified in core-negative hepatocytes the average
318 amount of DDX6-containing P-bodies per cell area was similar to the one in core-
319 positive hepatocytes. In addition, as it has been observed previously [22], the 3D
320 reconstruction of HCV-infected hepatocytes showed HCV core proteins forming ring-
321 like structures that surround lipid droplets, the site of viral RNA encapsidation.
322 Opposite to studies in cell culture [8], DDX6 did not colocalize with HCV capsid
323 proteins (**Fig. 4B**).

324

325 **Discussion**

326 *In vivo* studies are essential to deeply understand the complex interaction of HCV with
327 the infected hepatocyte and the associated pathogenesis. In this manuscript we report
328 that HCV infection impairs P-body formation in hepatocytes from human livers
329 regardless of viral genotype, inflammation grade or whether the infection is recent or
330 long established. The observed alterations are HCV-specific since no significant P-body
331 reduction was observed in chronically HBV-infected patients or in patients with non-
332 viral related hepatic inflammatory changes. Furthermore, the number of P-bodies was
333 restored once the virus is eliminated by therapy strengthening the requirement of the
334 presence of HCV for P-body disruption to occur. Interestingly, the number of P-bodies

335 per hepatocyte was highly heterogeneous among individuals covering a wide range of
336 values in healthy donors, HBV-infected, and non-viral related liver inflammation
337 patients. Nonetheless, in HCV-infected patients this range was very narrow indicating
338 that HCV is a decisive factor in P-body formation.

339

340 An unexpected observation in our study was the heterogeneous composition displayed
341 by P-bodies *in vivo*. To our knowledge all previous P-body studies in somatic cells have
342 been assessed in cell lines. In these studies DDX6 and Dcp1, two core P-body
343 components widely-used to visualize P-bodies, colocalize [7]. However, in hepatocytes
344 from both healthy donors and HCV-infected patients no colocalization was observed,
345 while lymphocytes surrounding these hepatocytes showed clear colocalization patterns.
346 The variable P-body composition among cell types might reflect different cell
347 regulation requirements [23]. Currently, we do not know if this is a special feature of
348 hepatocytes or is extended to other cell types. Another observation in conflict with
349 previous cell culture data was the no colocalization of DDX6 with the viral core protein.
350 Ariumi *et al.* determined that DDX6, among other P-body components, were hijacked to
351 lipid droplets where they colocalize with the core protein from JFH1 HCV strain [8].
352 However, with Jc1 HCV strain we failed to observe this colocalization in cell culture
353 [7]. These conflicting results might reflect differences in the dynamicity of core and
354 DDX6 interactions. Finally, another interesting observation in hepatocytes is that
355 DDX6-containing and Dcp1-containing P-bodies behave differently under certain
356 conditions. In hepatocytes from HBV-infected patients the number of DDX6-containing
357 P-bodies was significantly increased relative to hepatocytes from healthy donors. In
358 contrast, hepatocytes from HBV-infected patients displayed a tendency to show lower
359 Dcp1-containing P-body numbers when compared to healthy donors. Although the
360 cause of these distinct behaviours remains unknown, they might reflect a specialization

361 in P-body granules. Together, the observed heterogeneity in P-body composition among
362 cell types and within a single cell opens a new level of complexity that might reflect
363 functional specializations and deserves further exploration.

364

365 The HCV-induced reduction in P-body numbers might have profound effects in the
366 biology of the cell. P-body components are in a dynamic equilibrium between their
367 granule and a soluble localization in the cytosol, thus a reduction in the number of P-
368 bodies results in an increase of cytosolic P-body components [24-26]. As P-body
369 components include multiple proteins that control decay and silencing of mRNAs, the
370 transcriptome and translome is expected to be deregulated and consequently gene
371 expression altered. In chronic infections, HCV-induced reduction in P-body numbers
372 would result in a long-term alteration of gene expression that might contribute to HCV-
373 associated pathogenesis. In line with this, overexpression of the core P-body component
374 DDX6 has been observed in hepatocellular carcinomas [18]. This overexpression is
375 expected to alter the P-body numbers.

376

377 How and why HCV infection induces P-body disruption is not completely understood.
378 Our data in hepatoma cell lines support the hypothesis that HCV disrupts P-bodies by
379 hijacking or modifying core P-body components required for P-body formation [7, 8].
380 Lsm1-7, Pat1 and DDX6 are three core P-body components with a major role in
381 decapping and decay of cellular mRNAs [27]. HCV needs these factors and redirects
382 them for a role in the viral life cycle to promote HCV RNA translation and replication
383 [14, 28]. At the same time, the subsequent P-body disruption might also benefit viral
384 reproduction since P-bodies have been involved in innate immune responses [16].
385 Intriguingly, *in vivo*, the HCV-induced reduction in P-bodies was similar in core-
386 positive and core-negative cells (**Fig. 4A**). Consequently, either very low and

387 undetectable HCV replication is enough to cause P-body disruption or HCV-infected
388 cells induce P-body disruption of surrounding cells by unknown mechanisms.
389 Interestingly, perturbed metabolic zonation in HCV-infected livers has been recently
390 related to this last scenario [29].

391 In summary, this is the first comprehensive analysis of P-body granules *in vivo* and a
392 direct demonstration of a link between a pathogenic condition and P-body alterations.
393 Incorporating P-bodies into the mechanistic framework of multifaceted disease traits
394 adds another level of complexity that should be considered to fully understand the
395 molecular events causing HCV-induced liver disease and other serious diseases.

396

397

398

399

400

401

402

403

404

405

406

407

408

409

410

411

412

413 **Acknowledgements**

414 We thank A. Meyerhans for critically reading the manuscript and for helpful discussions
415 and T. Pengo for his advice in the design of scripts to analyze the confocal datasets.

416

417

418

419

420

421

422

423

424

425

426

427

428

429

430

431

432

433

434

435

436

437

438

439

440 **References**

- 441 [1] Thomas DL. Global control of hepatitis C: where challenge meets opportunity.
442 Nature medicine 2013;19:850-858.
- 443 [2] Bartenschlager R, Lohmann V, Penin F. The molecular and structural basis of
444 advanced antiviral therapy for hepatitis C virus infection. Nature reviews Microbiology
445 2013;11:482-496.
- 446 [3] Lange CM, Jacobson IM, Rice CM, Zeuzem S. Emerging therapies for the
447 treatment of hepatitis C. EMBO molecular medicine 2014;6:4-15.
- 448 [4] Kato T, Furusaka A, Miyamoto M, Date T, Yasui K, Hiramoto J, et al. Sequence
449 analysis of hepatitis C virus isolated from a fulminant hepatitis patient. Journal of
450 medical virology 2001;64:334-339.
- 451 [5] Wakita T, Pietschmann T, Kato T, Date T, Miyamoto M, Zhao Z, et al.
452 Production of infectious hepatitis C virus in tissue culture from a cloned viral genome.
453 Nature medicine 2005;11:791-796.
- 454 [6] Keskinen P, Nyqvist M, Sareneva T, Pirhonen J, Melen K, Julkunen I. Impaired
455 antiviral response in human hepatoma cells. Virology 1999;263:364-375.
- 456 [7] Perez-Vilaro G, Scheller N, Saludes V, Diez J. Hepatitis C virus infection alters
457 P-body composition but is independent of P-body granules. Journal of virology
458 2012;86:8740-8749.
- 459 [8] Ariumi Y, Kuroki M, Kushima Y, Osugi K, Hijikata M, Maki M, et al. Hepatitis
460 C virus hijacks P-body and stress granule components around lipid droplets. Journal of
461 virology 2011;85:6882-6892.
- 462 [9] Aizer A, Brody Y, Ler LW, Sonenberg N, Singer RH, Shav-Tal Y. The
463 dynamics of mammalian P body transport, assembly, and disassembly in vivo.
464 Molecular biology of the cell 2008;19:4154-4166.

- 465 [10] Kedersha N, Stoecklin G, Ayodele M, Yacono P, Lykke-Andersen J, Fritzler
466 MJ, et al. Stress granules and processing bodies are dynamically linked sites of mRNP
467 remodeling. *The Journal of cell biology* 2005;169:871-884.
- 468 [11] Anderson P, Kedersha N. RNA granules: post-transcriptional and epigenetic
469 modulators of gene expression. *Nature reviews Molecular cell biology* 2009;10:430-
470 436.
- 471 [12] Decker CJ, Parker R. P-bodies and stress granules: possible roles in the control
472 of translation and mRNA degradation. *Cold Spring Harbor perspectives in biology*
473 2012;4:a012286.
- 474 [13] Erickson SL, Lykke-Andersen J. Cytoplasmic mRNP granules at a glance.
475 *Journal of cell science* 2011;124:293-297.
- 476 [14] Scheller N, Mina LB, Galao RP, Chari A, Gimenez-Barcons M, Noueirry A, et
477 al. Translation and replication of hepatitis C virus genomic RNA depends on ancient
478 cellular proteins that control mRNA fates. *Proceedings of the National Academy of*
479 *Sciences of the United States of America* 2009;106:13517-13522.
- 480 [15] Beckham CJ, Parker R. P bodies, stress granules, and viral life cycles. *Cell host*
481 *& microbe* 2008;3:206-212.
- 482 [16] Lloyd RE. Regulation of stress granules and P-bodies during RNA virus
483 infection. *Wiley interdisciplinary reviews RNA* 2013;4:317-331.
- 484 [17] Blanco FF, Sanduja S, Deane NG, Blackshear PJ, Dixon DA. Transforming
485 growth factor beta regulates P-body formation through induction of the mRNA decay
486 factor tristetraprolin. *Molecular and cellular biology* 2014;34:180-195.
- 487 [18] Iio A, Takagi T, Miki K, Naoe T, Nakayama A, Akao Y. DDX6 post-
488 transcriptionally down-regulates miR-143/145 expression through host gene
489 NCR143/145 in cancer cells. *Biochimica et biophysica acta* 2013;1829:1102-1110.

490 [19] Nakagawa Y, Morikawa H, Hirata I, Shiozaki M, Matsumoto A, Maemura K, et
491 al. Overexpression of rck/p54, a DEAD box protein, in human colorectal tumours.
492 *British journal of cancer* 1999;80:914-917.

493 [20] Bedossa P, Poynard T. An algorithm for the grading of activity in chronic
494 hepatitis C. The METAVIR Cooperative Study Group. *Hepatology* 1996;24:289-293.

495 [21] Schindelin J, Arganda-Carreras I, Frise E, Kaynig V, Longair M, Pietzsch T, et
496 al. Fiji: an open-source platform for biological-image analysis. *Nature methods*
497 2012;9:676-682.

498 [22] Mensa L, Perez-del-Pulgar S, Crespo G, Koutsoudakis G, Fernandez-Carrillo C,
499 Coto-Llerena M, et al. Imaging of hepatitis C virus infection in liver grafts after liver
500 transplantation. *Journal of hepatology* 2013;59:271-278.

501 [23] Jonas S, Izaurralde E. The role of disordered protein regions in the assembly of
502 decapping complexes and RNP granules. *Genes & development* 2013;27:2628-2641.

503 [24] Teixeira D, Sheth U, Valencia-Sanchez MA, Brengues M, Parker R. Processing
504 bodies require RNA for assembly and contain nontranslating mRNAs. *Rna*
505 2005;11:371-382.

506 [25] Eulalio A, Behm-Ansmant I, Schweizer D, Izaurralde E. P-body formation is a
507 consequence, not the cause, of RNA-mediated gene silencing. *Molecular and cellular*
508 *biology* 2007;27:3970-3981.

509 [26] Franks TM, Lykke-Andersen J. TTP and BRF proteins nucleate processing body
510 formation to silence mRNAs with AU-rich elements. *Genes & development*
511 2007;21:719-735.

512 [27] Arribas-Layton M, Wu D, Lykke-Andersen J, Song H. Structural and functional
513 control of the eukaryotic mRNA decapping machinery. *Biochimica et biophysica acta*
514 2013;1829:580-589.

515 [28] Jangra RK, Yi M, Lemon SM. DDX6 (Rck/p54) is required for efficient
516 hepatitis C virus replication but not for internal ribosome entry site-directed translation.
517 Journal of virology 2010;84:6810-6824.

518 [29] Moreau M, Riviere B, Vegna S, Aoun M, Gard C, Ramos J, et al. Hepatitis C
519 viral proteins perturb metabolic liver zonation. Journal of hepatology 2014.

520

521

522

523

524

525

526

527

528

529

530

531

532

533

534

535

536

537

538

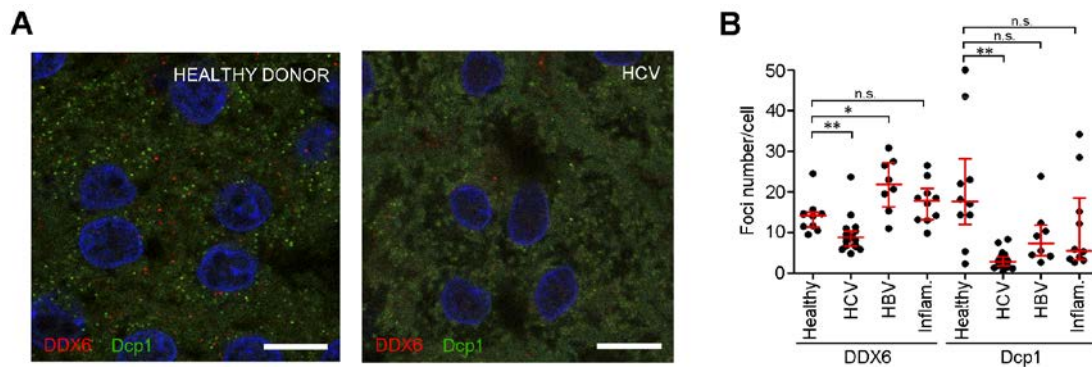
539

540

541

542 **Figures and Tables**

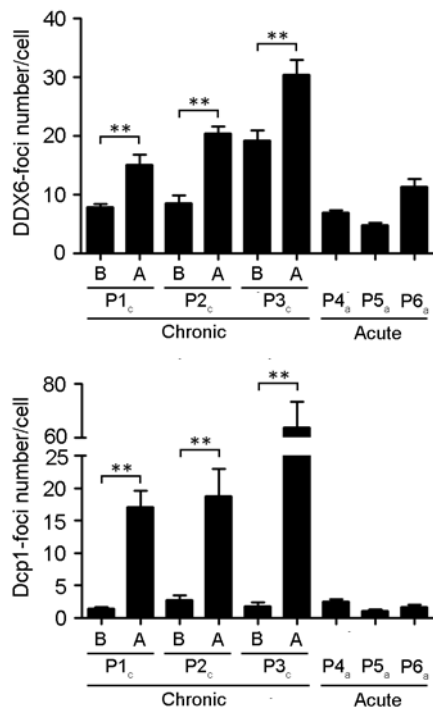
543 **Figure 1. HCV infection specifically decreases the number of P-bodies compared**
544 **with healthy donors.** Hepatic tissue was stained with antibodies to detect DDX6 (red)
545 and Dcp1 (green). Nuclei were visualized using DAPI (blue). (A) Representative
546 pictures from healthy donors and HCV-infected patients. Scale bar, 10 μ m. (B)
547 Quantification of DDX6- and Dcp1-containing P-bodies in healthy donors (Healthy,
548 n=10), HCV-infected (HCV, n=19), HBV-infected (HBV, n=8), and HCV-negative
549 patients with liver inflammation (Inflam., n=10). Dots indicate the median value per
550 biopsy, horizontal red lines indicate the median for each group of patients and vertical
551 red lines the interquartile range. Statistical significance was tested with Mann-Whitney
552 *U* test. **P* < 0.05; ***P* < 0.005; n.s., not significant.



553

554

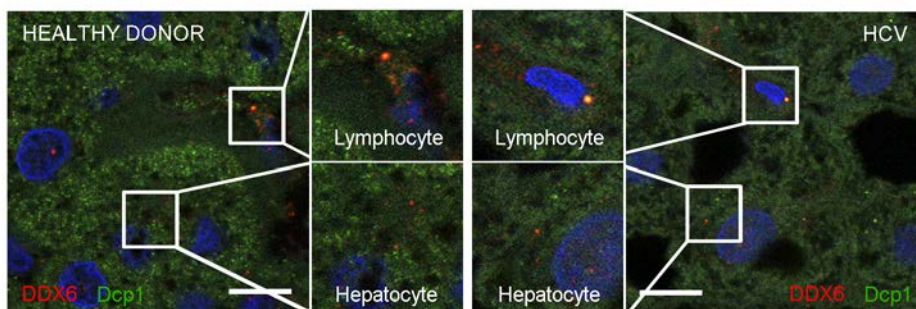
555 **Figure 2. P-body disruption occurs in acute and chronic HCV infections and is**
556 **reversed once HCV is eliminated.** Hepatic tissue was stained as described for Fig. 1A
557 and DDX6- and Dcp1-containing P-bodies were quantified in three HCV-chronic
558 infected patients (P1_c, P2_c and P3_c) before (B) and after (A) antiviral treatment, as well
559 as in three HCV-acute infected patients (P4_a, P5_a and P6_a). Displayed are the median
560 values for each patient, error bars indicate the standard error of the mean. Statistical
561 significance was tested with Wilcoxon test. ***P* < 0.005.



562

563

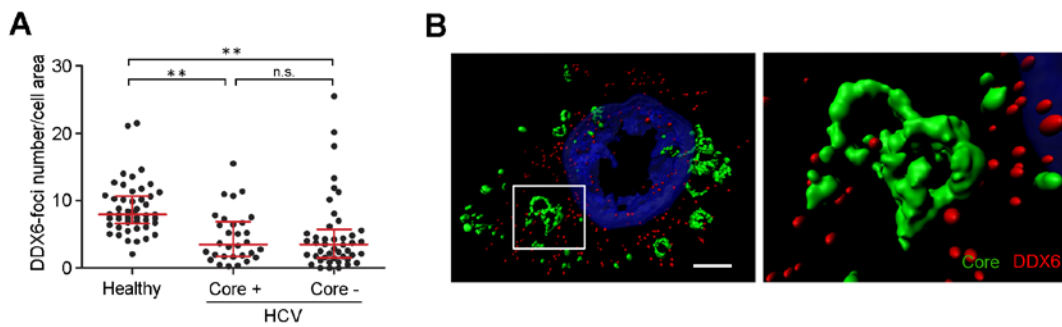
564 **Figure 3. Colocalization of DDX6 and Dcp1 in hepatocytes and parenchyma-**
 565 **infiltrating lymphocytes.** Hepatic tissue was stained in healthy donors and HCV-
 566 infected patients with antibodies to detect DDX6 (red) and Dcp1 (green). Nuclei were
 567 visualized using DAPI (blue). Scale bar, 10µm. Indicated areas in the images are
 568 magnified in the central columns.



569

570 **Figure 4. 3D single cell analysis validates DDX6-containing P-body decrease**
 571 **observed at a global level.** Hepatic tissue was stained with antibodies to detect DDX6
 572 (red) and the viral protein core (green). Nuclei were visualized using DAPI (blue). (A)

573 DDX6 P-body number was quantified at a single cell level along the Z-axis in healthy
574 donors (Healthy, n=4) and in HCV core-positive (Core +) and core-negative (Core -)
575 cells from HCV-infected patients (HCV, n=2). Horizontal red lines indicate the median
576 for each group of patients and vertical red lines show interquartile range. (B) Z-stack
577 images were 3D-segmented. Colocalization between both markers was assessed in
578 HCV-infected patients. Statistical significance was tested with Mann-Whitney *U* test.
579 ** $P < 0.005$; n.s., not significant. Scale bar, 3 μm .



580
581
582
583
584
585
586
587
588
589
590
591
592
593
594

595 **Table 1. Baseline characteristics of immunocompetent patients with chronic**
 596 **hepatitis C.** All patients (n= 19) were biopsied before treatment as clinically indicated
 597 in order to assess liver injury and fibrosis stage (METAVIR grade and stage,
 598 respectively). In this group, no specific association was found between P-bodies number
 599 and clinical parameters.

600

Patient	Age (years)	Gender (M/F)	HCV Genotype	Viral Load (log ₁₀ IU/mL)	AST/ ALT (IU/mL)	METAVIR grade	METAVIR stage
P1	35	M	4	5.22	71/155	A2	F2
P2	36	M	1b	5.97	33/48	A0	F0
P3	54	F	1a	5.24	71/54	A1	F2
P4	45	M	1b	5.01	30/36	A0	F0
P5	55	M	1b	5.05	152/203	A1	F4
P6	65	F	1b	5.79	73/94	A1	F2
P7	20	F	1b	4.40	66/158	A1	F2
P8	37	M	1b	6.04	114/262	A1	F2
P9	43	F	1b	5.18	67/138	A1	F1
P10	33	M	3	5.77	40/64	A2	F4
P11	55	F	1b	6.03	73/60	A1	F1
P12	23	F	1b	3.04	31/69	A1	F0
P13	51	M	1b	6.33	39/70	A0	F1
P14	66	M	1b	5.72	227/322	A2	F3
P15	55	M	1a	6.31	73/121	A2	F2
P16	29	M	4	5.17	39/45	A0	F0
P17	52	M	1b	6.72	144/196	A2	F4
P18	46	F	4	5.42	60	A1	F2
P19	47	M	2	2.33	45	A1	F2

601 M/F, male/female; AST, aspartate aminotransferase; ALT, alanine aminotransferase.

602

603

604

605

606 **Supplementary Table 1. Clinical characteristics among the control groups: healthy**
607 **donors, HBV-infected and HCV/HBV-negative LT patients with liver**
608 **inflammation.** All patients were biopsied as clinically indicated.

609

Patient ID	Control group	Age (years)	Gender (M/F)	IS	AST/ALT (IU/mL)	METAVIR stage	Histopathological diagnosis
P20	Healthy donors (n=10)	30	M	-	28/50	F0	Mild hemosiderosis
P21		30	M	-	21/18	F0	Mild hemosiderosis
P22		53	M	-	28/38	F0	Moderate hemosiderosis
P23		43	F	-	NA	F0	NAD
P24		54	F	-	NA/26	F0	Mild steatosis
P25		46	F	-	12/15	F0	NAD
P26		36	M	-	31/26	F0	Mild steatosis
P27		22	M	-	27/23	F0	Minimal changes
P28		28	M	-	25/33	F0	Mild hemosiderosis
P29		43	F	-	14/8	F0	NAD
P30	HBV (n=8)	27	M	-	231/574	F2	Suggestive of HBV infection
P31		40	M	-	31/44	F1	Suggestive of HBV infection
P32		49	F	-	53/60	F3	Suggestive of HBV infection
P33		37	M	-	48/68	F2	Compatible with HBV
P34		44	M	-	69/70	F3	Suggestive of HBV infection
P35		33	M	-	55/85	F2	Suggestive of HBV infection
P36		48	M	-	93/97	F3	Suggestive of HBV infection

P37		33	M	-	46/61	F1	Suggestive of HBV infection
P38	LT with inflammatory changes (n=10)	69	M	Other	52/73	F0	Steatohepatitis
P39		61	M	FK	11/25	F0	Rejection
P40		54	F	FK	22/20	F0	Unspecific inflammation
P41		31	F	CyS	55/215	F0	Rejection
P42		54	M	CyS	64/168	F1	Rejection
P43		59	M	FK	29/55	F0	Rejection
P44		38	M	FK	213/317	F0	Rejection
P45		69	M	FK	39/39	F0	Autoimmune hepatitis
P46		46	F	Other	43/53	F0	PBC recurrence
P47		67	M	CyS	100/88	F0	Rejection

610 LT, liver transplant; M/F, male/female; AST, aspartate aminotransferase; ALT, alanine aminotransferase;
611 IS, immunosuppression regimen; CyS, Cyclosporine A; FK, Tacrolimus; Other, mTOR inhibitor; PBC,
612 primary biliary cirrhosis; NAD, nothing abnormal detected.

613